

A Model organism approach: Defining the role of Neph proteins as regulators of neuron and kidney morphogenesis

Elke Neumann-Haefelin^{1§*}, Albrecht Kramer-Zucker^{1§}, Krasimir Slanchev¹, Björn Hartleben¹, Foteini Noutsou¹, Katrin Martin¹, Nicola Wanner^{1,6}, Alexander Ritter¹, Markus Gödel¹, Philip Pagel², Xiao Fu¹, Alexandra Müller³, Ralf Baumeister^{4,5}, Gerd Walz^{1,5} and Tobias B. Huber^{1,5,6*}

¹ Renal Division, University Hospital Freiburg, D-79106 Freiburg, Germany

² Lehrstuhl für Genomorientierte Bioinformatik, Technische Universität München, Munich, Germany

³ Department of Neuropathology, University Hospital Freiburg, D-79106 Freiburg, Germany

⁴ Bioinformatics and Molecular Genetics (Faculty of Biology) and ZBMZ Center for Biochemistry and Molecular Medicine (Faculty of Medicine), Albert-Ludwigs-Universität Freiburg, Germany

and FRIAS School of Life Sciences (LIFENET), Albert-Ludwigs-Universität Freiburg, Germany

⁵ Centre for Biological Signalling Studies (bioss), Albert-Ludwigs-Universität Freiburg, Germany

⁶ Spemann Graduate School of Biology and Medicine, University of Freiburg, Germany

§ These authors contributed equally to this work

*Address correspondence to:

Elke Neumann-Haefelin, MD

E-mail: elke.neumann-haefelin@uniklinik-freiburg.de

or

Tobias B. Huber, MD

Renal Division, University Hospital Freiburg

Breisacher Str. 66

D-79106 Freiburg

Germany

Phone: +49 761 270 3559

Fax: +49 761 270 3270

E-mail: tobias.huber@uniklinik-freiburg.de

Abstract

Mutations of the immunoglobulin superfamily proteins nephrin and Neph1 lead to congenital nephrotic syndrome in humans or mice. Neph proteins are three closely related molecules that are evolutionarily conserved and mediate cell recognition. Their importance for morphogenetic processes including the formation of the kidney filtration barrier in vertebrates and synaptogenesis in *C. elegans* has recently been uncovered. However, the individual morphogenetic function of mammalian Neph1-3 isoforms remained elusive. We demonstrate now that the Neph/nephrin family proteins can form cell-cell adhesion modules across species. Expression of all three mammalian Neph isoforms partially rescued mutant *C. elegans* lacking their Neph homolog *syg-1* and restored synapse formation, suggesting a functional redundancy between the three isoforms. Strikingly, the rescue of defective synaptic connectivity was prevented by deletion of the highly conserved cytoplasmic PDZ binding motif of SYG-1/Neph proteins indicating the critical role of this intracellular signaling motif for SYG-1/Neph-dependent morphogenetic events. To determine the significance of Neph isoform redundancy for vertebrate kidney development we analyzed the expression pattern and the functional role of Neph proteins in zebrafish. *In situ* hybridizations identified zNeph1 and zNeph2 as glomerular proteins. Morpholino knockdown of either *zNeph1* or *zNeph2* resulted in loss of slit-diaphragms and leakiness of the glomerular filtration barrier. This is the first report utilizing *C. elegans* to study mammalian Neph/nephrin protein function and to demonstrate a functional overlap of Neph1-3 proteins. Furthermore, we identify Neph2 as a novel critical regulator of glomerular function indicating that both Neph1 and Neph2 are required for glomerular maintenance and development.

Introduction

Glomerular podocytes form most complex three-dimensional epithelial structures and depend on a temporally and spatially precise tuning of cellular interactions (1). Immunoglobulin superfamily molecules interact with like molecules (homophilic interaction) and non-like molecules (heterophilic interaction) of neighboring podocytes to form a highly specialized cell-cell contact, the slit diaphragm, that regulates the positioning and dynamic interactions with other podocytes. The importance of immunoglobulin superfamily molecules like nephrin and Neph1 for the development and function of glomerular podocytes and the slit diaphragm is exemplified by the defects that have been discovered in mice and humans deficient in these molecules. Nephrin has been linked to congenital nephrotic syndrome in humans (2). Nephrotic Syndrome is characterized by increased permeability of the glomerular filtration barrier for macromolecules and renal failure. Although hereditary human diseases related to Neph proteins have yet to be identified, Neph1-deficient mice also show a severe congenital nephrotic syndrome (3). The cell-cell adhesion module formed by nephrin and Neph molecules serves not only as a guidepost for podocyte foot process formation and stability but does also impact the intracellular signal transduction machinery of podocytes in many ways (4).

The understanding of these dynamic signalling pathways involved in podocyte development and maintenance has been hampered by the low accessibility of mammalian podocytes *in vivo* and also by the difficulty to maintain fully differentiated podocytes in culture. In this respect, genetically tractable model organisms such as *Drosophila*, *C. elegans*, and zebrafish might contribute to the functional understanding of the highly conserved nephrin and Neph proteins.

Nephrin and Neph proteins are conserved through evolution. All Neph proteins share four to five extracellular immunoglobulin-like domains and a short cytoplasmic tail that contains a conserved PDZ

binding motif at the very carboxy terminus (5). The PDZ binding motif serves as scaffold for protein complex binding to facilitate intracellular signaling events (6). The extracellular domains of nephrin and Neph proteins bind to each other in *cis*- and/or *trans*- interactions (7) (8) (9). Two Neph1 (Roughest, Kirre) and two nephrin homologs (Hibris, Sticks-and-stones) are involved in pupal eye development and muscle fusion in *Drosophila* (10) (11) (12) (13). In *C. elegans*, synapse development and synaptic target recognition involves members of the nephrin-Neph protein family. The nephrin homolog SYG-2 and the Neph1 homolog SYG-1 mediate precise recognition of appropriate partners and trigger synapse formation of the hermaphrodite specific motor neuron (HSNL) (14, 15). The HSNL controls egg-laying behaviour by forming stereotypic *en passant* synapses on vulva muscle cells and ventral cord (VC) motor neurons. The recognition between HSNL and its targets and the precise positioning of synapses is initiated by adjacent vulva epithelial guidepost cells that express SYG-2/nephrin. SYG-2 interacts with SYG-1/Neph1 that is expressed in the HSNL, and thus recruits SYG-1 to the location along the HSNL axon where presynaptic sites are formed (14, 15). During development, transient presynaptic sites form at multiple locations along the HSNL axon. However, most of these presynaptic sites are eliminated by adulthood and only those where SYG-1 localizes remain (16).

C. elegans is easy genetically tractable and thus might be a promising model system to study general principles of nephrin-Neph protein functions and gain inside into the genetic network of podocytes. However, the system will also have limitations studying the functional role of nephrin-Neph molecules in the context of glomerular filtration.

The zebrafish pronephros model has had a significant impact on the understanding of renal development and disease (17). Although simple in form, the zebrafish pronephric glomerulus is composed of all cell types that are typical of higher vertebrate kidneys, including fenestrated endothelial cells in capillary tufts and podocytes with extensive foot processes that form the basket-like sieve

around the capillaries. The slit diaphragm molecules nephrin and podocin are highly and specifically expressed in pronephric podocytes and are required for the proper development of pronephric podocyte cell structure (18) (17). The zebrafish pronephros model therefore represents an ideal model to study the dynamics of foot process development.

Here, we for the first time combine *C. elegans* and zebrafish model systems to evaluate Neph protein function. Strikingly, all members of the mammalian Neph protein family are able to drive synapse formation in *C. elegans* motor neurons, demonstrating a general functional overlap of all Neph proteins and SYG-1. Lack of the highly conserved cytoplasmic PDZ binding motif of SYG-1 however, resulted in defective synaptogenesis indicating that SYG-1 morphogenetic processes involve intracellular signal transduction. Despite their functional overlap, Neph1 and Neph2 can not compensate for each other as a functional back-up mechanism for glomerular maintenance and development and we identify Neph2 as a novel critical regulator of the glomerular filtration barrier.

Results

The Neph protein family serves as an evolutionary conserved cell recognition module.

The assembly of cell contacts and development of synaptic specificity of the hermaphrodite specific motor neuron (HSNL) relies on heterophilic interactions between the *C. elegans* nephrin homolog SYG-2 located on vulva epithelial cells and the Neph1 homolog SYG-1 expressed in HSNL (14, 15). This asymmetric localization and interaction in *trans* configuration ensures presynapse formation in the HSNL at the appropriate location (Fig. 1A and B). In the mammalian kidney, however, it is hypothesized that interactions between nephrin and Neph proteins at the slit diaphragm may occur symmetrically in *cis* configuration as well as in *trans* configuration (Fig. 1B) (8). For an assessment of functional and phylogenetic relationships between the previously described Neph family members of *Caenorhabditis elegans* (*ce*), *Drosophila melanogaster* (*dm*), *mus musculus* (*mm*), *homo sapiens* (*hs*) and the 5 Neph sequences that we identified in zebrafish (*danio rerio*, *z*), we constructed protein trees based on observed sequence similarities by neighbor-joining (focussing on observed sequence similarity; Fig. 1C) and maximum likelihood (focussing on phylogenetic distance; Fig. 1D). Both trees largely agree on the overall topology. Evidently, subfamilies Neph1, Neph2, and Neph3 existed in the last common ancestor of the vertebrates represented in the analysis, causing these orthologous proteins to cluster together in the protein tree. The most notable exception from this agreement is the placement of zNeph2c (also referred as zNeph2). Depending on the choice of algorithm (neighbor-joining, maximum likelihood, UPGMA; not all data shown), parameters and protein domain, zNeph2c is placed at varying positions in the resulting tree. Based on its adjacency to the Neph2 family in Figure 1C and the previous annotation as Kirrel 3 (19), we chose to call the protein zNeph2c in this work. Nevertheless, we would like to stress that an unequivocal assignment to either of the subfamilies

remains speculation until additional sequences filling the gap become available or functional evidence resolves the issue. It is also conceivable that zNeph2c represents yet another family and thus belongs to none of the known groups.

Nephrin-Neph family proteins can form cell-cell adhesion modules across species.

Given the homology and structural similarity of the three mammalian Neph proteins we analyzed the capability of all Neph proteins to bind to nephrin. Previously we have cloned the closely related mammalian Neph1 proteins Neph2 and Neph3 (5) (Fig. 1C). The interaction between Neph1, Neph2, and nephrin has been characterized (7) (8) (9) (20). A series of co-immunoprecipitation experiments was performed after co-expressing epitope-tagged nephrin and Neph1-3 by transient transfection of human embryonic kidney (HEK) 293T cells. We confirmed that all three Neph proteins can interact with nephrin (Fig. 2A). Next, we investigated if this interaction is conserved between species. Indeed, SYG-2, the *C. elegans* homolog of nephrin, co-precipitated with Neph1-3 but not with the control protein RGS3 (Fig. 2B). Moreover SYG-1, homologous to Neph1, could be shown to interact with nephrin (Fig. 2C). In addition, a direct interaction between nephrin and SYG-2 could be demonstrated (Fig. 2D). These protein interactions could be confirmed by immunoprecipitation in both ways (Supplementary Fig. 1). Together, these observations indicated that the nephrin and Neph homologs share a high structural similarity and the formation of the Neph-nephrin complex is conserved across species.

Expression of mammalian Neph1 can rescue defective synaptogenesis in syg-1 mutant C. elegans.

Based on the structural redundancy of nephrin and Neph proteins of different species we tested the functional relationship between mouse Neph1 and *C. elegans* SYG-1. In adult wild-type worms, the HSNL forms synapses onto vulva muscles and VC motor neurons exclusively near the vulva region.

These synapses can be visualized *in vivo* using the vesicle marker synaptobrevin, SNB-1::YFP fusion (Fig. 3A). *syg-1(ky652)* null mutants have defects in synaptic specificity, synaptic vesicle markers in the HSNL axon fail to accumulate at normal synaptic locations and instead mislocalize to ectopic sites anterior to the vulva slit (Fig. 3B) (14) (16).

To gain insight into whether mNeph1 can complement *syg-1* function and guide synapse formation, we tested whether expression of mNeph1 in HSNL can rescue the synaptic phenotype of *syg-1* mutants. Therefore, we constructed transgenic worms containing the coding region of mNeph1 under control of an *unc-86* promoter which confers expression in HSNL. Strikingly, using independent transgenic lines, we found that mNeph1 rescued the synaptic vesicle defect of *syg-1(ky652)* mutants (Fig. 3D and E). SNB-1::YFP-labeled vesicles were partially redistributed to the HSNL axon segment near the vulva opening where synapses form. The fluorescence intensity of the marker was increased near the vulva compared to *syg-1(ky652)* mutants. However, expression of full length *syg-1* under control of the *unc-86* promoter more efficiently rescued the defective synaptogenesis of *syg-1* mutants (Fig. 3C and E). In agreement with the mNeph1 rescue experiments, mNeph1 fused to GFP exhibited correct localization to the presynaptic sites, at the points of contact between the guidepost cells expressing SYG-2 and the HSNL axon near the vulva, in a manner similar to SYG-1 (Fig. 3F). These findings suggest that mNeph1 can be recruited to appropriate location on the HSNL probably by interacting with SYG-2 expressed in guidepost cells. Furthermore, Neph1 can induce synapse formation indicating functional complementarity between *C. elegans* SYG-1 and mammalian Neph1 in synaptogenesis.

All mammalian Neph proteins (Neph1-3) display a functional overlap and can restore synaptogenesis in *syg-1* mutant *C. elegans*.

Our biochemical data indicated that Neph2, and Neph3, like Neph1, can form a complex with the *C. elegans* nephrin homolog SYG-2 (Fig. 2A and B). Therefore, we tested whether mouse Neph2 and Neph3 also have the capability to replace SYG-1 and to restore synapse formation at appropriate location near the vulva. We expressed mNeph2 and mNeph3 respectively in HSNL driven by the *unc-86* promoter in *syg-1(ky652)* mutants. Analysis of independent transgenic lines revealed that expression of mNeph2 or mNeph3 in *syg-1* mutants restored positioning of SNB-1::YFP-labeled vesicles near the vulva (Fig. 4D - F). However, as for mNeph1, the relocalization of synaptic vesicles from ectopic sites to the vulva was incomplete. Together, these results suggest that all mammalian Neph proteins share functions with *C. elegans* SYG-1 in synaptogenesis. Our findings identify *C. elegans* as a promising genetic model to study cell recognition and dynamic signalling events driven by the evolutionary conserved nephrin and Neph immunoglobulin superfamily. To our knowledge these are the first data using the model organism *C. elegans* to study mammalian podocyte molecules *in vivo*.

PDZ binding motif is important for SYG-1/Neph1 functions.

Next we utilized the *C. elegans* model to identify the functional role of a highly conserved intracellular Neph protein domain. All Neph proteins share a class 1 PDZ binding motif at their carboxy terminus (Fig. 5A). We previously identified specific protein interactions at this PDZ binding motif (6, 21). However, the *in vivo* function of the PDZ binding motif remained elusive. To test the importance of this protein motif we tried to rescue the *syg-1(ky652)* null mutants (Fig. 5D) with either wild-type protein or the deletion mutant lacking the three amino acid PDZ binding motif (*syg-1 Δ THV*) (Supplementary Fig.

2A). Whereas full length *syg-1* efficiently restored synaptic connectivity at normal sites in *syg-1* mutants (Fig. 5E and G), we found that expression of *syg-1 Δ THV* in *syg-1(ky652)* mutants did not result in a proper redistribution of the synaptic vesicles at appropriate sites (Fig. 5F and G). The correct localization of *syg-1 Δ THV* was demonstrated with the GFP fusion protein SYG-1 Δ THV::GFP (Fig. 5B). Like in *C. elegans* synapses, deletion of the PDZ binding motif seemed not to alter the localization of SYG-1 to the plasma membrane of HeLa cells (Supplementary Fig. 2B and C). Together, these findings suggest that morphogenetic processes controlled through Neph proteins can not only be attributed to adhesive mechanisms, but also involve intracellular signal transduction pathways specifically mediated by the cytoplasmic PDZ binding motif.

Neph1 and Neph2 are required for podocyte development.

In order to understand the significance of Neph isoform redundancy for vertebrate kidney development we analyzed the expression pattern and the functional role of Neph proteins in zebrafish. We identified five homologs of the human Neph proteins in zebrafish encoded by five different genes. Two (zNeph1a and zNeph1b) are related to hNeph1, another three (zNeph2a, zNeph2b and zNeph2c) share sequence similarities with hNeph2 (Fig. 1C). zNeph2c is also called zebrafish Kirrel, and was previously identified by another group as a homolog of Kin-of-IrreC (Kirre) and Roughest (Rst) and plays an important role in myoblast fusion (19). Out of the five members of the zebrafish Neph family identified, only zNeph1b and zNeph2c (hereafter referred to as zNeph1 and zNeph2 respectively) were expressed in the zebrafish larval kidney. Besides expression in the brain and other organ primordia, they were expressed in podocyte precursors in the glomerular primordium of the zebrafish pronephros beginning at 24 to 30 hpf when the primordia are still separated and at later stages in podocytes of the fused

glomerulus in the midline (Fig. 6A and B). zNeph1 and zNeph2 showed a similar distribution pattern as the podocyte proteins podocin and nephrin (18).

Considering the homology of Neph proteins of different species we next analyzed the capability of zebrafish Neph proteins to interact with nephrin. By immunoprecipitation from HEK 293T cells we could demonstrate that zNeph1 and zNeph2 bind to mammalian nephrin as well as the *C. elegans* homolog SYG-2 (Supplementary Fig. 3). Together, these observations underline the high phylogenetic similarity of Neph proteins and indicate that the Neph-nephrin complex formation is conserved inter species.

Disruption of protein function of zNeph1 and zNeph2 was done by injection of antisense morpholino oligonucleotides targeting splice donor sites of exons coding for the transmembrane domain. RT-PCR analysis of *Neph1* morpholino injected embryos revealed reduced *Neph1*mRNA levels but normal *Neph2*mRNA. Likewise, in *Neph2* morphant larvae *Neph2*mRNA was strongly reduced while *Neph1*mRNA remained unaffected indicating that *Neph1* and *Neph2* morpholinos specifically targeted their corresponding mRNA (Supplementary Fig. 4). Furthermore, upon knockdown of Neph proteins no alteration of the *nephrin*mRNA was detected. The *Neph1* and *Neph2* morphant phenotype was characterized by pericardial edema that often impairs blood circulation, and slight dorsal bending of the body axis (Fig. 7A - C). Pericardial edema was also seen in *podocin* and *nephrin* morphant larvae (18). On histological sections the architecture of the glomeruli seemed slightly disturbed and the adjacent ducts were dilated (Fig. 7B and C). The morpholino effect was quantified (Fig. 7G). Electron microscopy confirmed disrupted podocyte ultrastructure with foot process effacement and lack of fine interdigitation and slit-diaphragms in z*Neph1* and z*Neph2* morphant podocytes at 96 hpf (Fig. 7E and F) compared to the evenly spaced podocyte foot processes with connecting slit diaphragms in wild-type

podocytes (Fig. 7D). By analogy with the *nephrin* and *podocin* morphant larvae these abnormalities imply impaired function of the glomerular filter apparatus (18).

Impairment of the glomerular filter was further evaluated by a blood/urine barrier assay using injection of fluorescently labeled dextran (Fig. 8). Previous experiments have determined that dextran with MW 70 kDa can penetrate the kidney barrier and is found in the urine within several minutes post injection (18). In contrast, larger dextran molecules, 500 kDa, are prevented from entry into the urine of larvae with intact blood/urine barrier (18). Strikingly, whereas 100% of the wild-type larvae injected with 500 kDa FITC-dextran kept the fluorescent dye in the blood circulation, in around 30% of the examined morpholino injected embryos the barrier failed and the dye was found in the lumen of the pronephric duct (Fig. 8 A and B). Noteworthy, this assay is applicable only to larvae with sufficient blood flow which was impaired in many larvae injected with *Neph* morpholinos (see above). Therefore, at 84 hpf only larvae with milder phenotype were used for the assay which, together with the traditional limitations of the visual evaluation allowing detection only above a certain threshold, might explain the relatively low percentage (around 30%) of affected larvae. Nevertheless, leakage of the glomerular filter was only seen in morphant larvae.

Discussion

The overall architecture of podocyte networks is defined by the creation of highly specific cell-cell connections, the slit diaphragms. Formation, differentiation, navigation, and plasticity of podocyte foot processes all require tightly regulated cell-cell interactions between podocytes (1). Genetic studies have identified nephrin and Neph1 immunoglobulin superfamily proteins as essential components for the formation of the slit diaphragm and glomerular integrity (2). In addition, several other slit diaphragm adhesion molecules potentially capable of mediating slit diaphragm interactions have been identified (22). However, the functional role of each of these adhesion molecules and their signalling properties is still only partially understood. The fact that highly conserved nephrin-Neph molecules serve as cell-cell recognition modules in different settings in different species prompted us to utilize model organisms to study mammalian slit diaphragm proteins.

Our biochemical results illustrated a remarkable evolutionary plasticity in molecular interactions between mammalian, zebrafish, and *C. elegans* nephrin-Neph proteins, spanning 800 million years of evolution. Therefore, we sought to test the *C. elegans* system by functionally expressing mammalian Neph proteins in HSNL neurons of *C. elegans*. The *C. elegans* HSNL system seemed exceptionally well suited for heterologous nephrin-Neph expression given that the Neph1 homolog SYG-1 is the neuronal receptor for the nephrin homolog SYG-2 on adjacent epithelial cells to provide positional cues for synapse target selection and synaptogenesis (14, 15). Worms mutant for either *syg-1* or *syg-2* fail to target the HSNL synapses properly, indicating that the combined action of SYG-1/Neph1 and SYG-2/nephrin is needed to organize neuronal circuitry. In addition, the HSNL synapse system is organized in a more simple and predictable manner than the slit diaphragm due to the fact that SYG-1 and SYG-2 are asymmetrically located and the interactions seem to appear only in *trans*. Strikingly, we could

demonstrate that the heterologous expression of all three mNeph proteins functionally compensated for the loss of *syg-1* in HSNL synapses. This is a remarkable finding for several reasons: First, only a few heterologous expression experiments with mammalian homologs rescuing for the functional loss of their *C. elegans* homologs have been described before. Second, to ensure a functional rescue of a transmembrane protein like SYG-1, the heterologous molecule does not only need to bind the physiological ligands, but also requires to precisely localize to the predetermined cell surface and has to ensure the proper intracellular signalling pathways. Contact-mediated mechanisms of SYG-1/Neph are prerequisite but not sufficient for synaptic specificity of the HSNL, as an unrelated immunoglobulin protein did not rescue the *syg-1* mutant defective synaptogenesis (23). Neph1 and Neph2 are highly expressed in the mouse central nervous system and Neph1 localized to dendrites and synapses in the striatum (24). This expression pattern might point to a possible role for mammalian Neph proteins in synapse formation, but their precise function still needs to be defined. The system for heterologous expression of functional Neph proteins in *C. elegans* described here will provide a novel approach of carrying out structure function studies on nephrin-Neph molecules. In this respect, we could demonstrate that deletion of the highly conserved C-terminal PDZ binding motif in SYG-1 resulted in the inability to restore synaptic connectivity in the *syg-1* mutant underlining the critical importance of the cytoplasmic signalling functions of Neph molecules. For future studies, the easy traceable formation of HSNL synapses will be a powerful platform to apply reverse genetic screens identifying regulators important for SYG-1/Neph protein trafficking, localization, and signalling in *C. elegans* nervous system as well as the kidney slit diaphragm.

In contrast to *C. elegans*, that appears to express only a single isoform of Neph proteins, vertebrates express several closely related Neph isoforms (5). Thus, with the shown functional redundancy of Neph1-3 proteins, it is an important question whether these isoforms can function as a

back up or if they have distinct expression patterns, suggesting similar but not necessarily overlapping functions. Previously, we have identified the three closely related mammalian Neph proteins Neph1, Neph2, and Neph3 (5). Neph1-3 molecules seem to have partially overlapping expression patterns in neuronal tissue and all of the Neph proteins have been shown to localize at the slit diaphragm in glomerular podocytes (25) (9) (20) (26) (24) (27). Genetic deletion of *Neph1* resulted in renal failure and early postnatal lethality indicating that glomerular Neph2 and Neph3 can not compensate for the loss of Neph1 (3). This lack of compensation could point to differences in protein function, but could also be just the result of lowering the critical total amount of Neph proteins at the slit diaphragm needed to guide and maintain podocyte foot processes. Thus, the glomerular role of Neph isoforms other than Neph1 has remained unclear.

To resolve this issue, we identified five homologs of human Neph proteins in zebrafish vertebrate model and tested their expression and glomerular function. Interestingly, two (zNeph1 and zNeph2) out of the five members of the zebrafish Neph family were expressed in the zebrafish pronephric kidney. zNeph1 and zNeph2 showed a similar temporal and spatial expression pattern as the podocyte proteins podocin and nephrin (18). In agreement with the knockout of *Neph1* in mice, genetic interference with *zNeph1* in zebrafish caused severe podocyte alteration and foot process effacement. Strikingly, morpholino knockdown of *zNeph2* also resulted in an obvious kidney failure evidencing the functional importance of Neph protein isoforms other than Neph1 for kidney development and glomerular maintenance. Given the homology of Neph proteins and the structural similarity between the pronephros and the mammalian kidney these data strongly suggest that Neph protein isoforms will also be critical glomerular determinants in mice and human kidneys. However, future genetic mouse studies will have to confirm the importance of Neph2 and Neph3 for glomerular development.

Our *in silico* data suggested that the multiple Neph isoforms in vertebrates belong to three paralogous groups which have evolved before or during the emergence of early vertebrates. As gene duplication removes selective pressure from copies, these events frequently result in diverging non-redundant biological functions of the paralogs over the course of evolution and non-overlapping protein functions are not unlikely. Indeed, our data underline that the general function of the common ancestor appear to be conserved (as evidenced by the ability of all mammalian Neph isoforms to rescue the *syg-1*-deficient phenotype) and the lack of compensation of different Neph isoforms for each other in zebrafish podocytes might be interpreted as a diversification of Neph protein function.

Glomerular diseases are primarily responsible for end-stage renal disease worldwide. Due to its molecular complexity, the podocyte slit diaphragm protein machinery represents a main target for acquired and genetic diseases and is probably the most fragile component of the filtration barrier. The establishment of innovative techniques and models to overcome the difficult accessibility to study podocyte molecules *in vivo* will be a pacemaker to track molecular functions of slit diaphragm molecules and to identify novel therapeutic targets. Here, we for the first time combine *C. elegans* and zebrafish model systems to evaluate Neph protein function. All members of the mammalian Neph protein family display their functional overlap by their capability of driving synapse formation in *C. elegans* motor neurons. Despite this functional overlap, Neph1 and Neph2 are both needed for glomerular maintenance and we identify Neph2 as another essentially required immunoglobulin superfamily protein for the maintenance of the complex glomerular architecture.

Materials and methods

Multiple Alignments and construction of phylogenetic trees

Multiple protein sequence alignments were generated using MUSCLE v3.7 (28). Based on these alignments, phylogenetic trees were reconstructed with two different methods. Protein sequence similarity trees were built with the neighbor-joining algorithm without correcting for multiple substitutions using clustalx (29) (30). Maximum-likelihood trees, representing evolutionary distance, were built with the potml program of the phylib suite (31). The resulting trees were rooted using the *C. elegans* protein (SYG-1) as an outgroup. Rooting, tree-arrangement, and visualization was done with phylib's retree and drawgram tools, respectively. Used protein sequences were: ceSyg1 (Uniprot B1Q236), dmKirre (Uniprot Q9W4T9), dmC-Rst (Uniprot Q08180), hsNeph1 (Uniprot Q96J84), mmNeph1 (Uniprot Q80W68), hsNeph2 (Uniprot Q8IZU9), mmNeph2 (Uniprot Q8BR86), hsNeph3 (Uniprot Q6UWL6), mmNeph3 (Uniprot Q7TSU7), zNeph1a (Uniprot Q6NY23), zNeph1b (NCBI XP_694545), zNeph2a (NCBI XP_700618.3), zNeph2b (Ensembl ENSDARP00000080814), zNeph2c (Uniprot A5JTW0).

C. elegans strains

The strains used were as follow: wild-type N2 Bristol, *kyIs235 [Punc-86::snb-1::yfp;Punc-4::lin-10::dsred;Podr-1::dsred]*, CX652 *kyIs235;syg-1(ky652)*, *kyIs288 [Punc-86::syg-1::gfp;Podr-1::dsred]*.

Strains were maintained using standard methods at 20°C.

C. elegans transgenic lines

kyIs235;syg-1(ky652);Ex[Punc-86::syg-1;Pmyo-2::gfp], *kyIs235;syg-1(ky652);Is[Punc-86::mNeph1;Pmyo-2::gfp]*, *kyIs235;syg-1(ky652);Is[Punc-86::mNeph2;Pmyo-2::gfp]*, *kyIs235;syg-1(ky652);Is[Punc-86::mNeph3;Pmyo-2::gfp]*, *Ex[Punc-86::mNeph1::gfp;Pmyo-2::gfp]*. *kyIs235;syg-1(ky652);Ex[Punc-86::syg-1ΔTHV;Pmyo-2::gfp]*, *Ex[Punc-86::syg-1ΔTHV::gfp;Pmyo-2::gfp]*.

Molecular biology

For expression of *mNeph1*, *mNeph2*, and *mNeph3* in *C. elegans* driven by the *unc-86* promoter in HSNL the mouse full length cDNA was PCR amplified and cloned into *NheI* and *NcoI* sites of pSM (14). To express GFP-tagged *mNeph1* driven by the *unc-86* promoter in HSNL the full length *mNeph1* cDNA without stop codon was PCR amplified and cloned into the C-terminal GFP pSM vector (14). The *Punc-86::syg-1ΔTHV* construct was created by inserting the *syg-1* cDNA without the PDZ binding motif (the last three amino acids of the carboxy-terminal tail) under control of the *unc-86* promoter in pSM. A GFP-fusion protein of SYG-1 lacking the PDZ binding motif was generated by cloning *syg-1* cDNA without the THV motif into the C-terminal GFP pSM vector. To create N-terminally epitope-tagged constructs of *mNeph1-3*, *zNeph1*, *zNeph2*, *Nephrin*, *SYG-1*, and *SYG-2* the leader sequence of CD5 followed by the V5- or Flag-tag was fused to the 5' end of the coding sequence without the original leader sequence (6).

Transgenic C. elegans lines and fluorescence microscopy

To create transgenic animals expressing *mNeph1* fused to *gfp*, *Punc-86::mNeph1::gfp* plasmid was injected into the gonad of wild-type worms at a concentration of 5 ng/μl along with *Pmyo-2::gfp* (10

ng/ μ l) as co-injection marker. For *syg-1* Δ THV::*gfp* transgenic animals, *Punc-86::syg-1* Δ THV::*gfp* was injected at a concentration of 10ng/ μ l along with *Pmyo-2::gfp*. For rescue experiments of *syg-1* mutants, plasmids were injected into CX652 worms at a concentration of 5 ng/ μ l along with *Pmyo-2::gfp* (10 ng/ μ l) as co-injection marker. Extrachromosomal arrays of mNeph1, mNeph2, and mNeph3 respectively were integrated into the genome to help mitigate their genetic instability, mosaicity, and variability. The integration of the arrays was achieved by irradiation with 3000 Rad from a ¹³⁷Cesium source. The integrated lines were backcrossed at least eight times with wild-type N2 and crossed into CX652. Multiple independent transgenic lines were analyzed for the expression pattern of SNB-1::YFP and rescue of the *syg-1* mutant phenotype. HSNL vesicle cluster were visualized in young adult *kyIs235* animals with a Zeiss Axioplan2 microscope and an AxioCam camera.

RNA isolation and RT-PCR

RNA was isolated from approximately 100 worms at young adult stage using RNeasy Mini Kit (Qiagen) following the manufacturer's instructions and digested with DNase (RNase-Free DNase kit, Quiagen). cDNA synthesis was made using Superscript III RT (Invitrogen) and oligodT primer. PCR experiments were performed on 5x dilutions of the cDNA and the following primer pairs *syg-1*f: 5'-GTATCAGCTTCACTCGATG-3', *syg-1*r: 5'-CTTCTGCACATGCAGAGGCAG-3', *act-1*f: 5'-ATGTGTGACGACGAGGTTGC-3', *act-1*r: 5'-TAGATTGGGACGGTGTGGGT-3'. PCR products were then visualized on an agarose gel stained with ethidium bromide.

Cell culture and transfections

HEK 293T cells were cultured in DMEM supplemented with 10% FBS. For transfection experiments, cells were grown until 60–80% confluence and transfected with plasmid DNA using a modified calcium phosphate method as described previously (32).

Co-Immunoprecipitation

Co-immunoprecipitations were performed as described (32). Briefly, HEK 293T cells were transiently transfected. After incubation for 24 hours, cells were washed twice and lysed in a 1% Triton X-100 lysis buffer. After centrifugation (15,000xg, 15 min, 4°C) and ultracentrifugation at 100,000xg (30 min, 4°C) cell lysates containing equal amounts of total protein were incubated for 1 hour at 4°C with the appropriate antibody, followed by incubation with 20 µl of protein G-sepharose beads for approximately 1 hour. The beads were washed extensively with lysis buffer. Bound proteins were resolved by 10% SDS-PAGE and analyzed by immunoblot. Antibodies were obtained from Sigma (anti-FLAG M2 mAb) and Serotec (anti-V5 mAb).

Immunofluorescence

Hela cells were transfected with sV5.SYG-1 and sV5.SYG-1ΔTHV expression vectors using Lipofectamin (Invitrogen). Cells were incubated with anti-V5 rabbit polyclonal antibody (Milipore). After washing with DMEM cells were fixed with 4% paraformaldehyde and incubated with Alexa Fluor 488-conjugated secondary antibody anti-rabbit. Images were taken using a Zeiss Apotome equipped with a 63x water immersion objective.

Zebrafish lines and cloning of members of the Neph family in zebrafish

Wild-type AB and ABTL zebrafish were maintained and raised as described (18). Dechorionated embryos were kept at 28.5°C in Danieau's solution with or without 0.003% PTU (1-Phenyl-2-thiourea, Sigma) to suppress pigmentation and staged according to hours post fertilization (hpf) (18). For the dextran assay, transgenic zebrafish larvae expressing mCherry protein in the pronephric duct under the control of a NaK-ATP-ase subunit promoter were used (A.K.Z. and K.S., unpublished data). Zebrafish *Neph* fragments and full length cDNA were amplified from 48 hpf total RNA by RT-PCR. The primer were designed based on sequence predictions of tblastn searches from Sanger Center zebrafish genomic DNA sequence (Sanger Institute, Cambridge UK, <http://www.ensembl.org/Multi/blastview>). The following primer pairs were used: zNeph1b-f outer 5'-GAGTCCGGCGTAAAGAAGATGAAT-3'; zNeph1b-r outer 5'-TATTTGCGTTCAAGGAAGTGCTTT-3'; zNeph1b-f inner 5'-CGACGCGTACCATGGGCTTCAGCATGACC-3'; zNeph1b-r inner 5'-AAATATGCGGCCGCTCACACATGAGTCTGCAT-3'; zNeph2c-f outer 5'-GACAAGTGTTGAAGACTCCGGAAA-3'; zNeph2c-r outer 5'-TGCTTAATCCCTCCTGAACCAGAT-3'; zNeph2c-f inner 5'-CGACGCGTACCATGTTGGCGTTTTACATC-3'; zNeph2c-r inner 5'-AAATATGCGGCCGCTCACACGTGAGTCTGCAT-3'.

In situ hybridization

Whole-mount in situ hybridization was performed as previously described (18). The antisense riboprobes were generated using a *Bam*HI linearized templates subcloned in pCS2+ and T7 RNA polymerase. Embryos were hybridized with digoxigenin-labeled riboprobes. Anti-DIG AP (1:5000) and the NBT/BCIP substrate (Boehringer Mannheim) were used to detect the probe. After the color reaction

was stopped, embryos were cleared in 100% glycerol and photographed using a stereomicroscope (Leica MZ16).

Morpholino antisense oligonucleotide injections

Injections were performed as previously described (18). Briefly, wild-type embryos at the 1 to 2 cell stage were microinjected with antisense morpholino oligonucleotides (Gene Tools LLC) diluted in 100 mM KCL, 0.1% Phenol Red and 10mM HEPES, pH 7,5. The morpholino oligonucleotides were designed to target a splice donor site of a coding exon in the transmembrane domain. The sequence for *Neph1b* morpholino (MO) was 5'AAACAGATACACTCACACATAAACC3' and for *Neph2c* morpholino 5'ATCTGACCTTTGGCCTCACCTTTAG3'. The morpholino effects were verified by nested PCR with primers amplifying the full-length cDNA (see above). A fragment of the zebrafish nephrin mRNA was amplified to check the expression level, the following primer pair was used: zNephrin-f 5'-CATCAACCAAGTTACCCGTTACCA-3', zNephrin-r 5'-TGAAGGGTTAAGGCCTGTGACTGTA-3' (according to (18)). RT-PCR was performed from total RNA of single embryos (72 hpf). For histology analysis, larvae were fixed in 4% PFA in PBS, embedded with Technovit 7100 resin (Kulzer, Germany), and sectioned at 5 µm thick sections. Sections were then stained with hematoxylin and eosin.

Fluorescent dextran assay

A transgenic fishline Na,K-ATPase alpha1A:4mCherry (promoter described in (33)) was used. 84 hpf old wild-type or morpholino injected anesthetized zebrafish larvae, from the NaK:mCherry line, were injected with 1% Lysine-fixable FITC-dextran (500 kDa, Molecular Probes) fluorescent dye dissolved in PBS pH 7.4, directly into the common cardinal vein (18). After an incubation period of 3 hours, the

larvae were mounted in 1,5% low melting agarose and examined using confocal microscopy (ZEISS LSM510 Axioplan) for the presence of fluorescent dextran in the lumen of the pronephric duct. Only embryos with blood circulation, as judged by sufficiently moving blood cells, were used for these barrier assay experiments.

Transmission electron microscopy

Zebrafish larvae were fixed in 3% glutaraldehyde in Sørensen's buffer (100 mM, pH 7.45) at 4 °C over night. They were then rinsed in Sørensen's buffer (100 mM, pH 7.45) and post-stained in 1% osmium tetroxide with $K_4(Fe(CN)_6)$ for 6 h at RT and rinsed in distilled water. This was followed by stepwise dehydration through a graded series of ethanol and propylene oxide: The larvae were infiltrated in a 2:1 solution of propylene oxide and Epon Araldite (Serva) for 1.5 h, then in a 1:2 solution of propylene oxide and Epon Araldite for 2 h at RT, and finally infiltrated in pure Epon Araldite for 4 h at 40 °C, embedding was done at 70 °C over night. Thin sections (50-70 nm) were cut on a Reichert Ultracut S ultramicrotome and collected onto copper grids (200 Mesh Sq Fine Bar). The sections were stained with uranyl acetate and lead citrate and examined in a Philips CM100 TEM at 80 kV.

Acknowledgements

We thank Charlotte Meyer, Dörte Thiel, Nelli Schetle, Lara Schomas, and Alexandra Schwierzok for excellent technical assistance. We thank Alexandra Müller and Christine Kremer for the excellent technical assistance with the electron microscopy. We thank K. Shen (Department of Biological Sciences, Stanford University, Stanford CA) for *Punc-86::syg-1* dpSM plasmid and the *Caenorhabditis* Genetics Center for worm strains. This study was supported by DFG grants to E.N.H. (KFO 201); A.K.Z. (SFB 592 and KFO 201); R.B. (SFB592, KFO201, bioss EXC294 and EC 6th Framework Network of Excellence LIFESPAN (LSHG-CT-2007-036894), and T.B.H. (HU 1016/2-1, SFB 592 and KFO 201) and by the Excellence Initiative of the German Federal and State Governments (EXC 294).

Disclosures

None.

References

1. Simons, M., Hartleben, B. and Huber, T.B. (2009) Podocyte polarity signalling. *Curr Opin Nephrol Hypertens*, **18**, 324-330.
2. Tryggvason, K., Patrakka, J. and Wartiovaara, J. (2006) Hereditary proteinuria syndromes and mechanisms of proteinuria. *The New England journal of medicine*, **354**, 1387-1401.
3. Donoviel, D.B., Freed, D.D., Vogel, H., Potter, D.G., Hawkins, E., Barrish, J.P., Mathur, B.N., Turner, C.A., Geske, R., Montgomery, C.A. *et al.* (2001) Proteinuria and perinatal lethality in mice lacking NEPH1, a novel protein with homology to NEPHRIN. *Mol Cell Biol*, **21**, 4829-4836.
4. Huber, T.B. and Benzing, T. (2005) The slit diaphragm: a signaling platform to regulate podocyte function. *Curr Opin Nephrol Hypertens*, **14**, 211-216.
5. Sellin, L., Huber, T.B., Gerke, P., Quack, I., Pavenstadt, H. and Walz, G. (2003) NEPH1 defines a novel family of podocin interacting proteins. *Faseb J*, **17**, 115-117.
6. Hartleben, B., Schweizer, H., Lubben, P., Bartram, M.P., Moller, C.C., Herr, R., Wei, C., Neumann-Haefelin, E., Schermer, B., Zentgraf, H. *et al.* (2008) Neph-Nephrin proteins bind the Par3-Par6-atypical protein kinase C (aPKC) complex to regulate podocyte cell polarity. *J Biol Chem*, **283**, 23033-23038.
7. Barletta, G.M., Kovari, I.A., Verma, R.K., Kerjaschki, D. and Holzman, L.B. (2003) Nephrin and Neph1 co-localize at the podocyte foot process intercellular junction and form cis heterooligomers. *J Biol Chem*, **278**, 19266-19271.
8. Gerke, P., Huber, T.B., Sellin, L., Benzing, T. and Walz, G. (2003) Homodimerization and heterodimerization of the glomerular podocyte proteins nephrin and NEPH1. *J Am Soc Nephrol*, **14**, 918-926.
9. Liu, G., Kaw, B., Kurfis, J., Rahmanuddin, S., Kanwar, Y.S. and Chugh, S.S. (2003) Neph1 and nephrin interaction in the slit diaphragm is an important determinant of glomerular permeability. *J Clin Invest*, **112**, 209-221.
10. Strunkelnberg, M., Bonengel, B., Moda, L.M., Hertenstein, A., de Couet, H.G., Ramos, R.G. and Fischbach, K.F. (2001) *rst* and its paralogue *kirre* act redundantly during embryonic muscle development in *Drosophila*. *Development*, **128**, 4229-4239.
11. Dworak, H.A., Charles, M.A., Pellerano, L.B. and Sink, H. (2001) Characterization of *Drosophila hibris*, a gene related to human nephrin. *Development*, **128**, 4265-4276.
12. Dworak, H.A. and Sink, H. (2002) Myoblast fusion in *Drosophila*. *Bioessays*, **24**, 591-601.
13. Ramos, R.G., Igloi, G.L., Lichte, B., Baumann, U., Maier, D., Schneider, T., Brandstatter, J.H., Frohlich, A. and Fischbach, K.F. (1993) The irregular chiasm C-roughest locus of *Drosophila*, which affects axonal projections and programmed cell death, encodes a novel immunoglobulin-like protein. *Genes Dev*, **7**, 2533-2547.
14. Shen, K. and Bargmann, C.I. (2003) The immunoglobulin superfamily protein SYG-1 determines the location of specific synapses in *C. elegans*. *Cell*, **112**, 619-630.
15. Shen, K., Fetter, R.D. and Bargmann, C.I. (2004) Synaptic specificity is generated by the synaptic guidepost protein SYG-2 and its receptor, SYG-1. *Cell*, **116**, 869-881.
16. Ding, M., Chao, D., Wang, G. and Shen, K. (2007) Spatial regulation of an E3 ubiquitin ligase directs selective synapse elimination. *Science*, **317**, 947-951.
17. Drummond, I.A. (2000) The zebrafish pronephros: a genetic system for studies of kidney development. *Pediatr Nephrol*, **14**, 428-435.

18. Kramer-Zucker, A.G., Wiessner, S., Jensen, A.M. and Drummond, I.A. (2005) Organization of the pronephric filtration apparatus in zebrafish requires Nephrin, Podocin and the FERM domain protein Mosaic eyes. *Dev Biol*, **285**, 316-329.
19. Srinivas, B.P., Woo, J., Leong, W.Y. and Roy, S. (2007) A conserved molecular pathway mediates myoblast fusion in insects and vertebrates. *Nat Genet*, **39**, 781-786.
20. Gerke, P., Sellin, L., Kretz, O., Petraschka, D., Zentgraf, H., Benzing, T. and Walz, G. (2005) NEPH2 is located at the glomerular slit diaphragm, interacts with nephrin and is cleaved from podocytes by metalloproteinases. *J Am Soc Nephrol*, **16**, 1693-1702.
21. Huber, T.B., Schmidts, M., Gerke, P., Schermer, B., Zahn, A., Hartleben, B., Sellin, L., Walz, G. and Benzing, T. (2003) The carboxyl terminus of Neph family members binds to the PDZ domain protein zonula occludens-1. *J Biol Chem*, **278**, 13417-13421.
22. Quaggin, S.E. and Kreidberg, J.A. (2008) Development of the renal glomerulus: good neighbors and good fences. *Development*, **135**, 609-620.
23. Chao, D.L. and Shen, K. (2008) Functional dissection of SYG-1 and SYG-2, cell adhesion molecules required for selective synaptogenesis in *C. elegans*. *Mol Cell Neurosci*, **39**, 248-257.
24. Gerke, P., Benzing, T., Hohne, M., Kispert, A., Frotscher, M., Walz, G. and Kretz, O. (2006) Neuronal expression and interaction with the synaptic protein CASK suggest a role for Neph1 and Neph2 in synaptogenesis. *The Journal of comparative neurology*, **498**, 466-475.
25. Kestila, M., Lenkkeri, U., Mannikko, M., Lamerdin, J., McCready, P., Putaala, H., Ruotsalainen, V., Morita, T., Nissinen, M., Herva, R. *et al.* (1998) Positionally cloned gene for a novel glomerular protein--nephrin--is mutated in congenital nephrotic syndrome. *Mol Cell*, **1**, 575-582.
26. Minaki, Y., Mizuhara, E., Morimoto, K., Nakatani, T., Sakamoto, Y., Inoue, Y., Satoh, K., Imai, T., Takai, Y. and Ono, Y. (2005) Migrating postmitotic neural precursor cells in the ventricular zone extend apical processes and form adherens junctions near the ventricle in the developing spinal cord. *Neuroscience research*, **52**, 250-262.
27. Ihalmo, P., Schmid, H., Rastaldi, M.P., Mattinzoli, D., Langham, R.G., Luimula, P., Kilpikari, R., Lassila, M., Gilbert, R.E., Kerjaschki, D. *et al.* (2007) Expression of filtrin in human glomerular diseases. *Nephrol Dial Transplant*, **22**, 1903-1909.
28. Edgar, R.C. (2004) MUSCLE: multiple sequence alignment with high accuracy and high throughput. *Nucleic acids research*, **32**, 1792-1797.
29. Thompson, J.D., Higgins, D.G. and Gibson, T.J. (1994) CLUSTAL W: improving the sensitivity of progressive multiple sequence alignment through sequence weighting, position-specific gap penalties and weight matrix choice. *Nucleic acids research*, **22**, 4673-4680.
30. Thompson, J.D., Gibson, T.J., Plewniak, F., Jeanmougin, F. and Higgins, D.G. (1997) The CLUSTAL_X windows interface: flexible strategies for multiple sequence alignment aided by quality analysis tools. *Nucleic acids research*, **25**, 4876-4882.
31. Felsenstein, J. (1988) Phylogenies from molecular sequences: inference and reliability. *Annual review of genetics*, **22**, 521-565.
32. Huber, T.B., Hartleben, B., Kim, J., Schmidts, M., Schermer, B., Keil, A., Egger, L., Lecha, R.L., Borner, C., Pavenstadt, H. *et al.* (2003) Nephrin and CD2AP associate with phosphoinositide 3-OH kinase and stimulate AKT-dependent signaling. *Mol Cell Biol*, **23**, 4917-4928.
33. Liu, Y., Pathak, N., Kramer-Zucker, A. and Drummond, I.A. (2007) Notch signaling controls the differentiation of transporting epithelia and multiciliated cells in the zebrafish pronephros. *Development*, **134**, 1111-1122.

Figure Legends

Fig. 1 Neph proteins of the immunoglobulin superfamily are evolutionary conserved and control cell-cell recognition events.

- A In *C. elegans*, synapse formation between the hermaphrodite specific motor neuron (HSNL) and its targets, the ventral cord (VC) neurons and vulval muscles, is mediated by cell contact with guidepost epithelial cells. Position of the vulva opening and HSNL in the midpart of *C. elegans* viewed from lateral side. Boxed blowup shows HSNL details in the vulva region. Anatomically approximate schematic showing HSNL and vulva morphology. In wild-type animals presynaptic components normally localize to the segment of HSNL axon that is in contact with guidepost cells which express SYG-2. In *syg-1* mutants synapses are displaced along the HSNL axon to ectopic sites anterior the vulva.
- B Left panel: asymmetric distribution of SYG-2 on epithelial guidepost cells and SYG-1 on the HSNL axon in *C. elegans* drives synapse formation.
Right panel: *cis* and *trans* localisation of nephrin and Neph proteins in podocyte foot processes of the mammalian kidney seems to be required to set up an intact slit diaphragm.
- C Protein tree of the Neph family based on sequence similarity (neighbor-joining). Neph proteins of the immunoglobulin superfamily are evolutionary conserved. Phylogenetic tree of Neph molecules from *Caenorhabditis elegans* (ce), *Drosophila melanogaster* (dm), zebrafish (z), mouse (mm), and human (hs). The topology suggests that the duplication leading to the formation of subfamilies 1, 2 and 3 happened early during (or before) the appearance of vertebrates.

- D Protein tree of the Neph family focussing on evolutionary distance (maximum likelihood). The overall topology is identical to 1C – only branch lengths and the placement of zNeph2c differ.

Fig. 2 Inter-species conservation of nephrin-Neph complex formation.

- A Mammalian nephrin interacts with all Neph family members in HEK 293T cells. V5.Nephrin and Flag-tagged Neph1, Neph2, or Neph3 were co-expressed in transiently transfected HEK 293T cells. Cellular lysates were incubated with anti-Flag antibody to precipitate Neph proteins. V5.Nephrin, bound to each of the Neph proteins, was detected by Western blot (WB) analysis using anti-V5 antibody. The control protein F.RGS3 failed to immobilize nephrin (upper panel). Middle panel shows expression of V5.Nephrin in the cell lysates, the lower panel shows the expression of Flag-tagged proteins.
- B *C. elegans* SYG-2 co-precipitates with mammalian Neph proteins. *C. elegans* V5.SYG-2 and mammalian Flag-tagged Neph proteins or RGS3 were expressed in transiently transfected HEK 293T cells. After immunoprecipitation with anti-Flag antibody, the immobilized SYG-2 was detected with anti-V5 antibody in the precipitate containing Neph1, Neph2, or Neph3, but not RGS3 (upper panel). Middle part shows expression of V5.SYG-2 in the cell lysates, the lower panel shows the expression of Flag-tagged proteins.
- C *C. elegans* SYG-1 interacts with mammalian nephrin. V5.SYG-1 and Flag-tagged Nephrin or RGS3 were expressed in HEK 293T cells. After immunoprecipitation with anti-Flag antibody, the immobilized SYG-1 was detected with anti-V5 antibody in the precipitate containing nephrin but not in the RGS3 precipitate (upper panel). Middle panel shows expression of V5.SYG-1, the lower panel the expression of Flag-tagged proteins.
- D *C. elegans* SYG-2 interacts with mammalian nephrin. Flag-tagged Nephrin was co-expressed with V5.SYG-2 and precipitated with anti-Flag antibody. V5.SYG-2 bound to nephrin was detected using anti-V5 antibody.

Fig. 3 Mammalian Neph1 can reconstitute defective synapse formation in *syg-1* *C. elegans* mutants.

- A - E Mammalian Neph1 can partially rescue defective synapse formation in *syg-1* mutants. Paired DIC (upper panel) and fluorescence (middle panel) images of the vulva region of representative young adult *kyIs235* animals expressing the synaptic vesicle marker synaptobrevin SNB-1::YFP in HSNL. Lower panel shows schematic representation of the DIC and fluorescence images above. Arrowhead indicates the location of HSNL cell body, asterisk the vulva. All images are lateral views, head is to the left and ventral is down. Scale bar indicates 20 μ m.
- A Wild-type worm expressing synaptic vesicle marker SNB-1::YFP in HSNL. Synaptic vesicles are clustered near the vulva.
- B In *syg-1(ky652)* mutants, synaptic vesicles are displaced anterior the vulva along the axon in HSNL.
- C The *syg-1* mutant synaptic vesicle defect can be rescued by expression of *syg-1* under the *unc-86* promoter which drives expression in HSNL. *syg-1(ky652);Ex[unc-86::syg-1]* animals show normal SNB-1::YFP synaptic vesicles positioned adjacent to the vulva, similar to wild-type animals.
- D Expression of mouse Neph1 in HSNL can partially rescue defective synaptogenesis in *syg-1* mutants. Full length *mNeph1* was expressed under control of the *unc-86* promoter in *syg-1(ky652)*. SNB-1::YFP vesicles are redistributed to the axon segment near the vulva.
- E Quantification of SNB-1::YFP-labeled synaptic vesicles in *syg-1(ky652)* mutants rescued by ectopically expressed SYG-1 and mNeph1. Percentage of worms with synaptic vesicles at ectopic locations. Quantification in the young adult stage, n>50 per strain. Error bars indicate standard error of the mean.

F GFP-tagged mNeph1 localizes to the synaptic region of HSNL near the vulva. DIC (lower panel) and fluorescence (upper panel) images of the vulva region of representative young adult animals, lateral view. Full length mNeph1 or SYG-1 was fused to GFP and expressed in HSNL using the *unc-86* promoter. Scale bar equals to 20 μ m.

Fig. 4 Conserved function of Neph family proteins in *C. elegans* synapse formation.

A - E Paired fluorescence (upper panel) and DIC (lower panel) images of the vulva region of representative young adult *kyIs235* animals expressing the synaptic vesicle marker synaptobrevin SNB-1::YFP in HSNL. All images are lateral views of *Is[unc-86::snb-1::yfp]*, head is to the left and ventral is down. Scale bar indicates 20 μ m.

- A In wild-type worms, SNB-1::YFP-labeled vesicles are confined to an axon segment near the vulva slit.
- B In *syg-1(ky652)* mutants, the accumulation of presynaptic vesicles near the vulva slit is reduced and synapses mislocalize anterior to the vulva along the HSNL axon.
- C The synaptic vesicle defect of *syg-1(ky652)* mutants can be rescued by transgenic expression of *syg-1* under the *unc-86* promoter.
- D Expression of *mNeph2* in HSNL can partially rescue defective synaptogenesis in *syg-1(ky652)* mutants. Full length *mNeph2* was expressed under control of the *unc-86* promoter in *syg-1(ky652)*.
- E Transgenic expression of *mNeph3* in *syg-1(ky652)* can partially relocalize synaptic vesicles to the axon segment near the vulva.
- F Quantification of worms with SNB-1::YFP-labeled synaptic vesicles in *syg-1(ky652)* mutants rescued by ectopically expressed mNeph2 and mNeph3. Percentage of worms with synaptic vesicles at ectopic locations. Quantification in the young adult stage, n>50 per strain. Error bars, standard error of the mean.

Fig. 5 PDZ binding motif is important for SYG-1/Neph functions.

- A The carboxy terminal tail of Neph proteins contains a class 1 PDZ domain binding motif (X-T-X-V), which is highly conserved among mouse Neph1-3, *C. elegans* SYG-1, and *D. melanogaster* Kire and C-Rst.
- B SYG-1 Δ THV localizes at presynaptic sites similar to SYG-1. DIC (upper panel) and fluorescence (lower panel) images of the vulva region of representative young adult animals, lateral view. *syg-1* or *syg-1* Δ THV lacking the PDZ binding motif were fused to GFP and expressed in HSNL using the *unc-86* promoter.
- C-F SYG-1 Δ THV lacking the cytoplasmic PDZ binding motif does not restore defective synapse formation in *syg-1* mutants. Paired DIC (upper panel) and fluorescence (middle panel) images of the vulva region of representative young adult *kyIs235* animals expressing the synaptic vesicle marker synaptobrevin SNB-1::YFP in HSNL. Lower panel shows schematic representation of the DIC and fluorescence images above. Arrowhead indicates the location of HSNL cell body, asterisk the vulva. All images are lateral views, head is to the left and ventral is down. Scale bar indicates 20 μ m.
- C In wild-type worms, SNB-1::YFP vesicles accumulate near the vulva.
- D In *syg-1(ky652)* mutants, presynaptic vesicles mislocalize anterior to the vulva along the HSNL axon.
- E The *syg-1* mutant synaptic defect can be restored by expression of *syg-1* driven by the *unc-86* promoter. *syg-1(ky652);Ex[unc-86::syg-1]* animals position SNB-1::YFP synaptic vesicles adjacent to the vulva, similar to wild-type animals.
- F Deletion of the PDZ binding motif in SYG-1 fails to rescue defective synaptogenesis in *syg-1* mutants. SYG-1 Δ THV lacking the cytoplasmic PDZ binding motif (last three amino acids) was

expressed in *syg-1(ky652)*. SNB-1::YFP vesicles are mislocalized to ectopic sites anterior to the vulva.

- G Quantification of SNB-1::YFP-labeled synaptic vesicles at ectopic locations in the young adult stage, n>50 per strain. Error bars, standard error of the mean.

Fig. 6 Neph proteins are expressed in the pronephric glomerulus in teleost fish.

A, B zNeph1 (A) and zNeph2 (B) are expressed in the pronephric glomerulus (arrows) and in parts of the brain. Both are expressed in the forming glomerulus starting at 24 to 30 hpf, they mark the podocyte precursor cells in the nephron primordia that are not fused in the midline yet. They continue to be expressed at 72 hpf and 96 hpf. Cross-sections at 72 hpf show the glomerular expression of zNeph1 and zNeph2 respectively, the localization is typical for podocytes (A and B, arrow) surrounding the glomerular capillary tuft (*) originating from the dorsal aorta. Spots of dark pigment in the trunk in the cross-section (A) are not Neph1 expressing cells but rather pigment cells that escaped PTU treatment.

Fig. 7 *Neph* morphant embryos exhibit pericardial edema, glomerular malformation and podocyte footprocess effacement.

A - C Morpholinos (MO) were designed to target the transmembrane domain of Neph1 and Neph2 respectively. *Neph1* and *Neph2* morphant larvae develop pericardial edema (arrowheads) and deviation of the body axis at 72 hpf compared to wild-type larvae (upper panels). Histological sections of 72 hpf embryos stained with hematoxylin/eosin (lower panels) show a normal glomerulus (star) in a wild-type larva (A) and glomeruli with slightly disturbed architecture and somewhat dilated ducts (white arrowheads) adjacent to the glomerulus (B, C). Scale bars correspond to 500 μm (upper panels) and 50 μm (lower panels).

D - F In contrast to wild-type podocytes where foot processes and slit-diaphragms appear as “beads on a string” (D; arrowheads) *Neph1* and *Neph2* morphant podocytes at 96 hpf show foot process effacement and lack of fine interdigitation and slit-diaphragms on electron micrographs (E and F). Scale bars correspond to 1 μm .

- G Quantification of the described phenotypes observed in 48 hpf zebrafish larvae upon injection of 1 nL of 1 mM *Neph1* and 0.75 mM *Neph2* morpholino oligonucleotides (uninjected, n=54; *Neph1* MO, n=78; *Neph2* MO, n=101). 95% of embryos injected with morpholino against *Neph1* showed mild pericardial edema. 31% of embryos injected with morpholino against *Neph2* developed a severe heart edema and impaired blood flow.

Fig. 8 *Neph* morphants show a disturbed glomerular barrier function.

- A Confocal images of the pronephric duct of living 84 hpf wild-type (first panel) or *Neph* morpholino (MO) injected embryos (panel 2 and 3), injected with 500 kDa FITC-dextran. Each panel is a single confocal plane image (2.3 μm thickness), where the pronephric duct cells are labeled in red and the dextran in green. White arrowheads show dextran signal in the lumen of the duct and in apical endocytic vesicles of duct cells of MO injected embryos (panels 2 and 3).
- B Quantification of the observed phenotype. Dextran was detected in the duct of about 30% of the morpholino injected embryos, in contrast to none of the wild-type embryos, implying impaired barrier function of the pronephric glomerulus.

The abbreviations used are:

syg, synaptogenesis abnormal; HSNL, hermaphrodite specific motor neuron; PDZ, PSD95/Dlg/ZO-1;

MO; morpholino

Figure 1

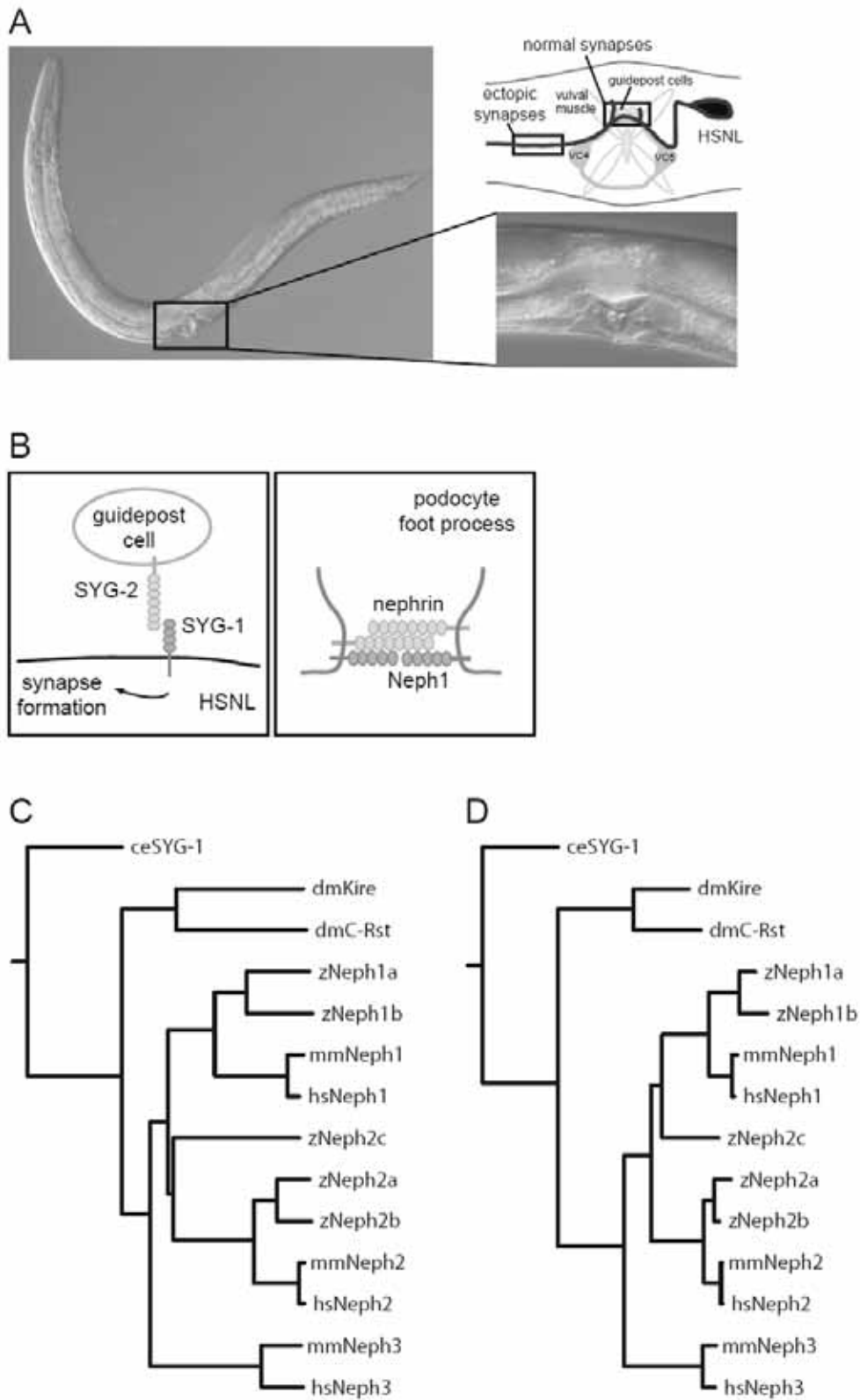


Figure 2

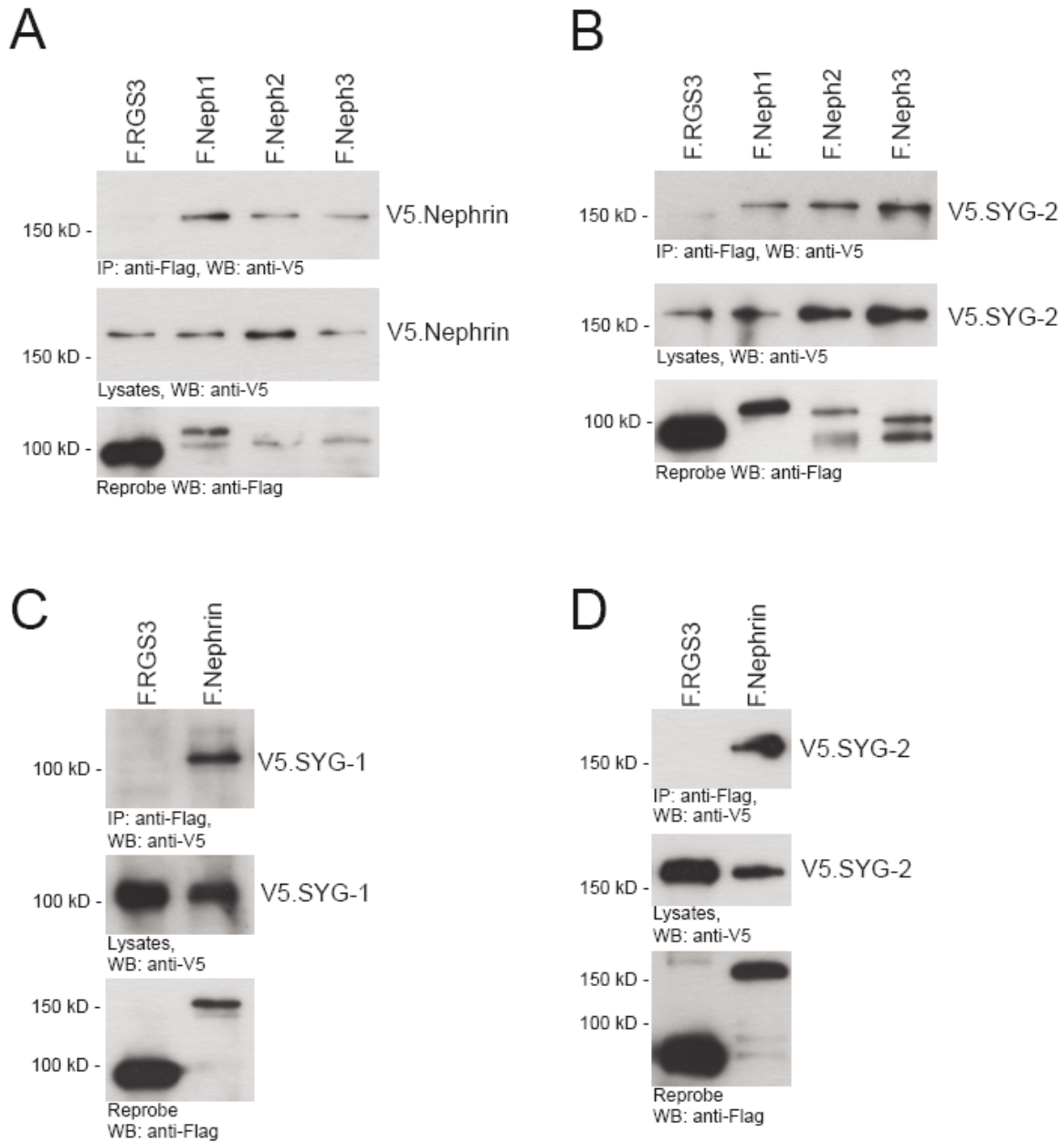


Figure 3

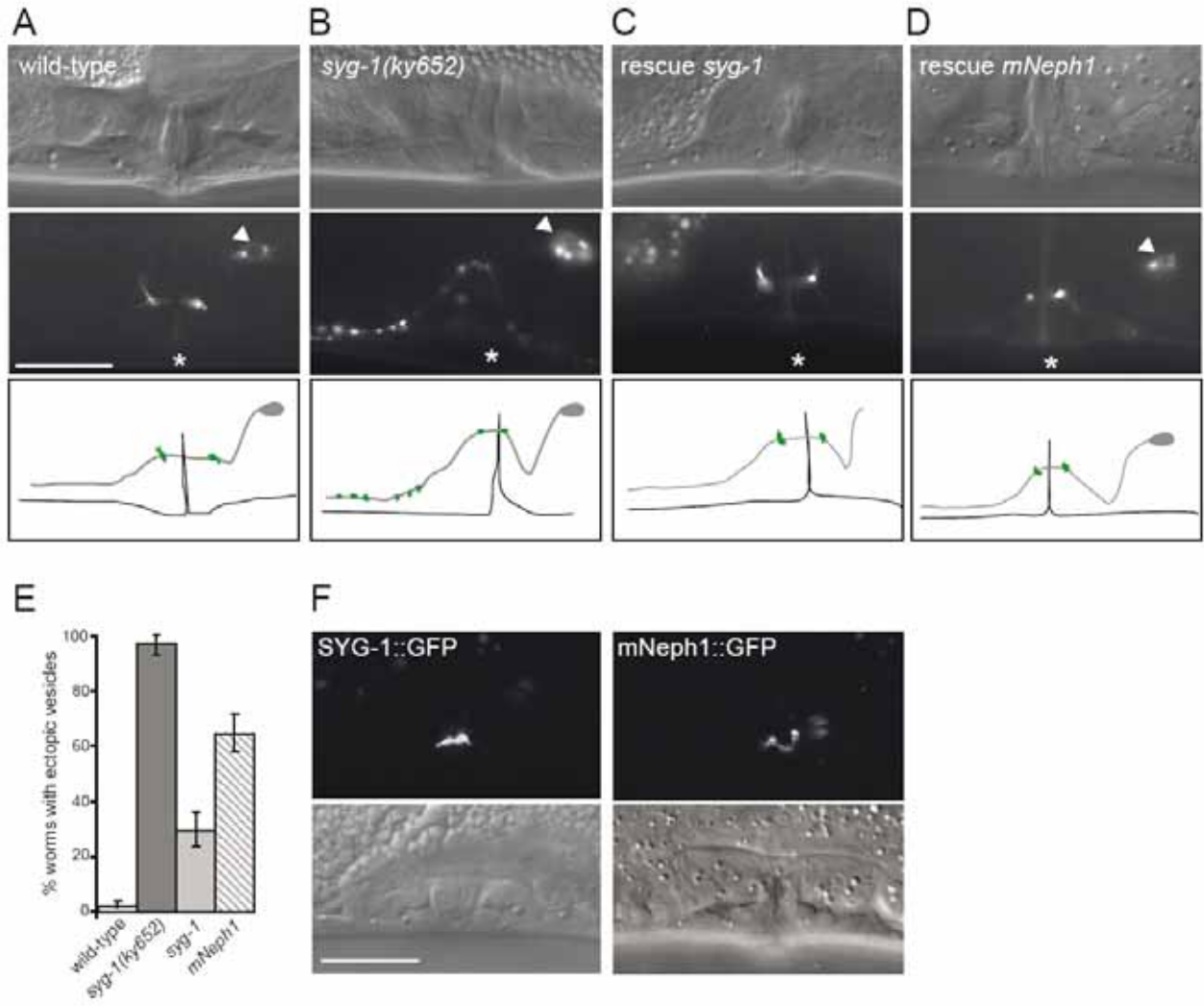


Figure 4

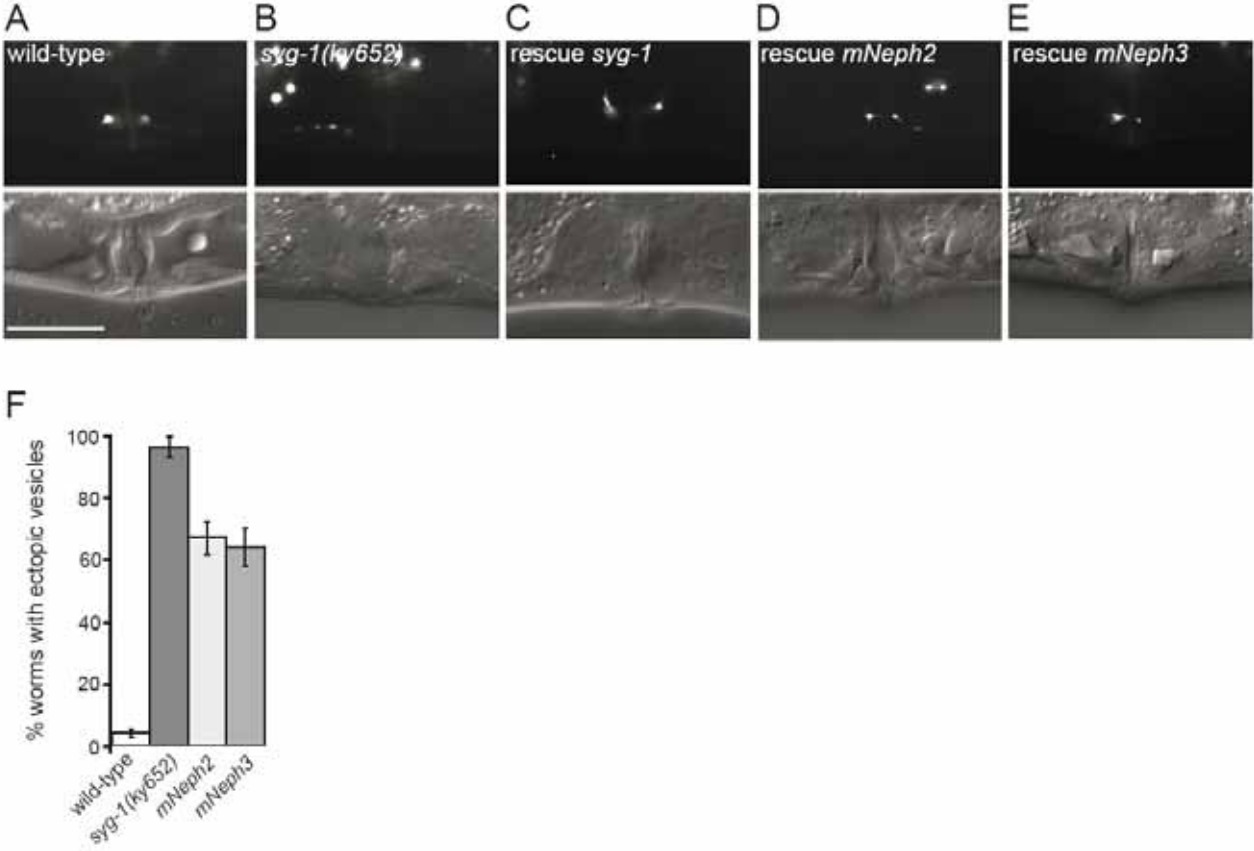


Figure 5

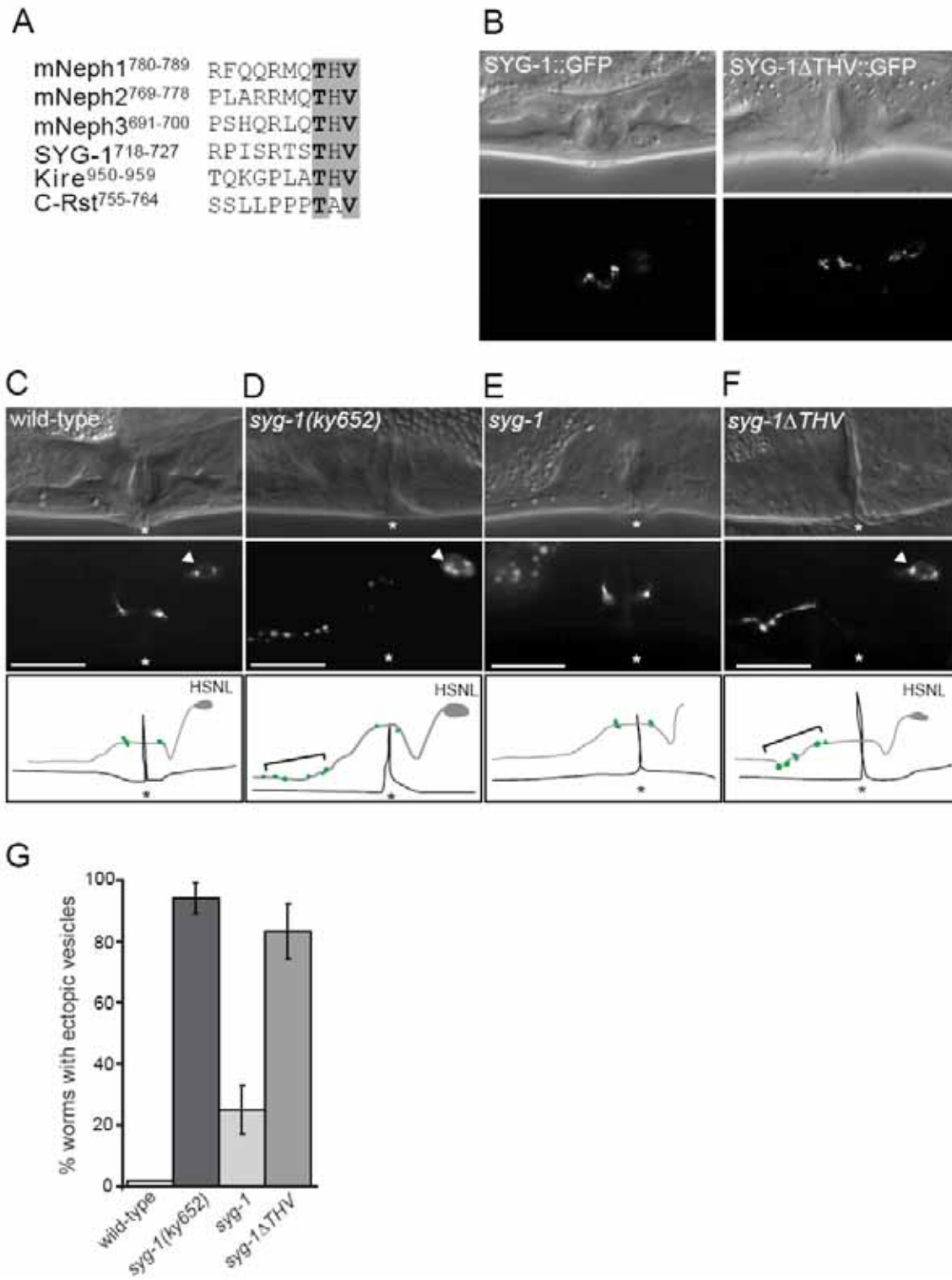


Figure 6

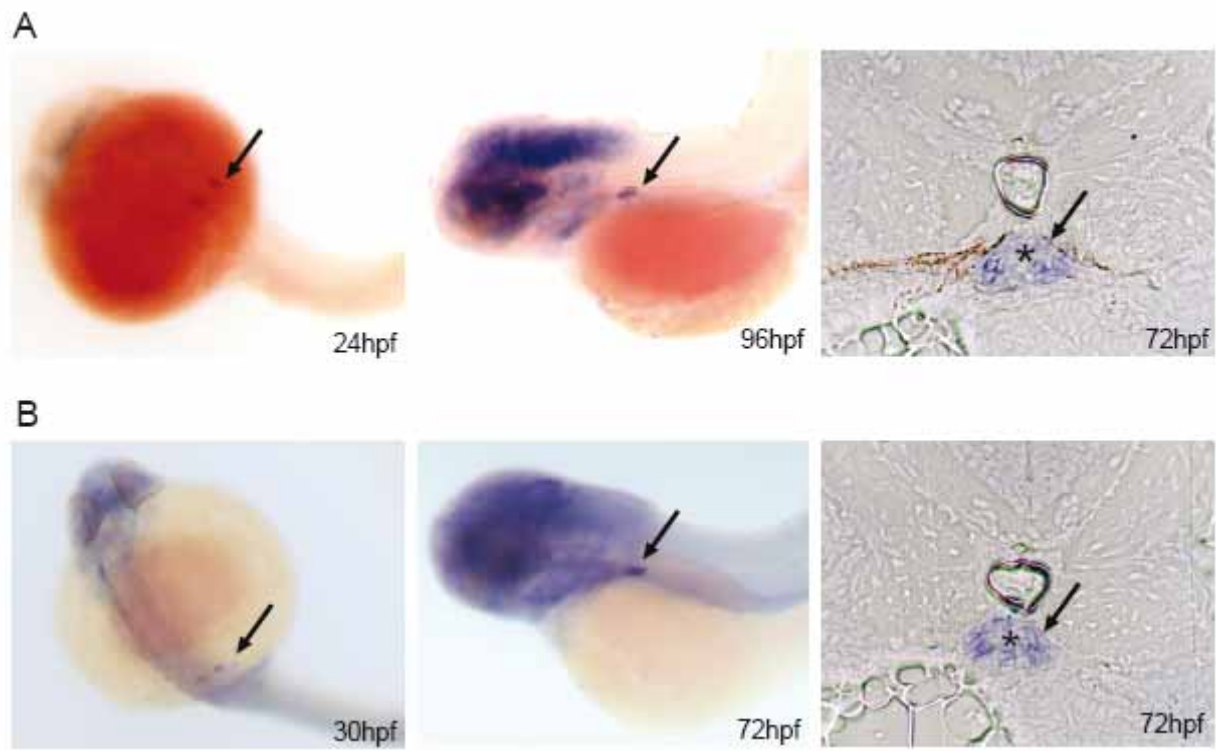


Figure 7

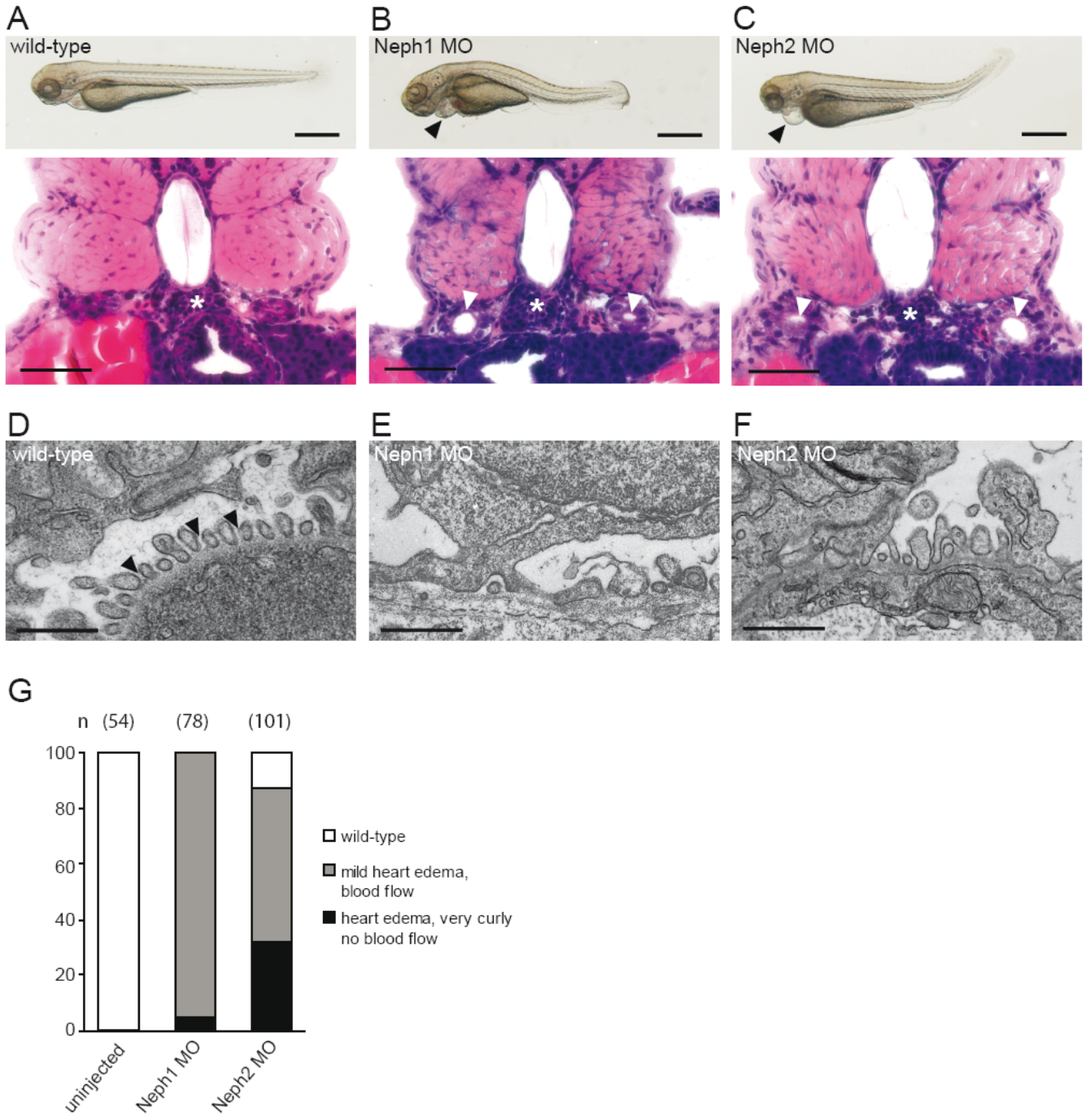


Figure 8

